AAEC/E345

AAEC/E345

AUSTRALIAN ATOMIC ENERGY COMMISSION

RESEARCH ESTABLISHMENT

LUCAS HEIGHTS

AN ANALYSIS OF POWER TRANSIENTS OBSERVED IN SPERT I REACTORS

PART 1 TRANSIENTS IN ALUMINIUM PLATE-TYPE REACTORS INITIATED AT AMBIENT TEMPERATURE

by

B. E. CLANCY

J. W. CONNOLLY

B. V. HARRINGTON

March 1975

ISBN 0 642 99677 6

AUSTRALIAN ATOMIC ENERGY COMMISSION

RESEARCH ESTABLISHMENT

LUCAS HEIGHTS

AN ANALYSIS OF POWER TRANSIENTS OBSERVED IN SPERT I REACTORS

PART 1 TRANSIENTS IN ALUMINIUM PLATE-TYPE REACTORS INITIATED AT AMBIENT TEMPERATURE

by

B. E. CLANCY

J. W. CONNOLLY

B. V. HARRINGTON

ABSTRACT

An investigation of SPERT I reactor reactivity feedback mechanisms has been made using the modular code AUS. Feedback terms so obtained have been used in the transient analysis code ZAPP to calculate transient behaviour for step and ramp reactivity additions. A simple model of coolant boiling has been used to analyse transients for which cladding temperatures exceed the saturation temperature of water.

The generally good agreement obtained with experimental data supports the case that core only temperature coefficients are much larger than those obtained by heating core and reflector.

National Library of Australia card number and ISBN 0 642 99677 6

The following descriptors have been selected from the INIS Thesaurus to describe the subject content of this report for information retrieval purposes. For further details please refer to IAEA–INIS–12 (INIS: Manual for Indexing) and IAEA–INIS–13 (INIS: Thesaurus) published in Vienna by the International Atomic Energy Agency.

A CODES; BOILING; FEEDBACK; REACTIVITY; REACTOR CORES; REACTOR KINETICS; SIMULATION; SPERT–1 REACTOR; TRANSIENTS VOID COEFFICIENT; Z CODES

CONTENTS

1. INTRODUCTION

In 1954, the USAEC initiated a theoretical and experimental program which had as its immediate objective the acquisition of a thorough understanding of the power transient behaviour of light water moderated, highly enriched uranium fuelled reactors. This class of reactor, in which the uranium fuel is usually dispersed in a flat plate of U–Al alloy and clad with aluminium, was then being constructed in large numbers to provide research facilities ranging from essentially zero power pool reactors to the materials testing reactor (MTR) and engineering test reactor (ETR).

This program, known as SPERT I, culminated in November 1962 with the planned destructive test on the D12/25 core. Between 1957 and that date, four other reactor cores had been subjected to transients covering the range of initial periods from 10 seconds to 10 milliseconds and clearly demonstrated the self–limiting properties of the power bursts.

Theoretical studies of the SPERT experiments have concentrated on moderator boiling as the principal shutdown mechanism (Forbes 1959, Turner 1968). Although those studies achieved some success in reproducing the main features observed in the SPERT transients, calculation of absolute values of reactor power required that normalisation to experimental data be employed. This, together with the inability of the calculations to reproduce correctly the course of transients in which cladding temperatures did not reach the saturation temperature of water, made it uncertain whether the feedback mechanisms had in fact been correctly identified.

The work reported here has placed prime emphasis on the calculation of non–boiling shutdown. This has led to the rejection of the static measurements of reactivity coefficients reported by Wing (1964) and Zeissler (1963) and the use instead of coefficients calculated by perturbation theory in a two–dimensional diffusion theory representation of the reactor core. Four SPERT cores have been analysed in this manner and generally good agreement has been obtained for non–boiling transients in the SPERT program. The calculated feedback coefficients have suggested a simple model for transients in which moderator boiling occurs. This model neglects void formation by steam bubbles, the boiling process only acting to increase the heat conduction from the fuel plate into the water. Good agreement has been obtained with experimental data by the use of this model.

2. GENERAL FEATURES OF SPERT TRANSIENTS

The analysis of reactor transient behaviour requires the solution of the usual point kinetic equations

$$\frac{dn}{dt} = \left(\frac{k(t)\ \{1-\beta\}-1}{\ell^*}\right) n + \Sigma\ \lambda_i\ C_i\ , \qquad (1)$$

$$\frac{dC_i}{dt} = \frac{k(t)\ \beta_i}{\ell^*}\ n - \lambda_i\ C_i\ , \qquad (2)$$

where the symbols have their usual meaning, and a third equation

$$k = f(s)\ , \qquad (3)$$

in which k is some function of the state of the system (s). If the state of the system is determined by the reactor power, P(t),Equation (3) provides a coupling between k and P. In general, the problem reduces to that of a correct identification of the coupling mechanism and the magnitude and sign of the feed–back coefficients.

The Nordheim–Fuchs equation, which has been found to provide a good description of power bursts in small, fast assemblies, is perhaps the simplest example of the coupling condi–

tions; delayed neutrons are ignored and the reactivity feedback is assumed to be directly proportional to the energy release. Thus,

$$\frac{1}{P}\frac{dP}{dt} = \alpha_o - b\,E \ ,$$

where α_o is the initial asymptotic inverse period following a step increase of reactivity. The solution of this equation predicts the following burst behaviour:

- Peak power (P_{max}) increases as α_o^2.
- The energy release E_{tm} to the time of peak power and the total energy release E_{tot} increase as α_o.
- P_{max}, E_{tm} and E_{tot} are inversely proportional to b, the energy coefficient of the instantaneous inverse period.
- The power pulse is symmetric, and $E_{tot} = 2\,E_{tm}$.
- The ratio $\alpha_o\ E_{tm}/P_{max} = 2$.
- Inclusion of delayed neutrons in this equation leads to a break in the plot of P_{max} *vs.* α_o in the region near prompt critical. In the region between prompt and delayed critical, P_{max} varies as α_o.

The SPERT transient power measurements showed that:

- P_{max} increases approximately as $\alpha_o^{1.7}$ for super prompt critical excursions.
- For transients in which cladding temperatures exceed the saturation temperature of water, the power pulse shape becomes markedly asymmetric with values of $E_{tot} \sim 1.5\,E_{tm}$.
- If the shutdown mechanism is assumed to be due solely to void and expansion effects and the energy partition between fuel plate and water is constant, then b is proportional to the void coefficient C_v divided by the prompt neutron lifetime. Comparison of results for cores with different values of C_v/ℓ^* indicated that P_{max} varied as $(\ell^*/C_v)^{1/2}$ rather than ℓ^*/C_v as predicted by the Nordheim–Fuchs equation.

These results led to a modification of Equation (4)

$$\frac{1}{P}\frac{dP}{dt} = \alpha_o - b\,E^n \ , \qquad (5)$$

the solutions of which give

$$P_{max} = \frac{\alpha_o^{\frac{n+1}{n}}}{b^{1/n}}\ \frac{n}{n+1} \qquad (6)$$

$$E_{tm} = \left(\frac{\alpha_o}{b}\right)^{1/n} \qquad (7)$$

$$E_{tot} = \left(\frac{\alpha_o}{b}\right)^{1/n}\ (n+1)^{1/n} \ . \qquad (8)$$

A good fit to the observed variation of these quantities with α_o was obtained for values of n between 1.7 and 2 for super prompt critical transients. The calculation of absolute quantities from Equations (6), (7) and (8) remained a difficulty, however, since the quantity dV/dE implicit in b is very large for steam produced voids. As noted by Forbes (1959), if heat transfer rates observed in steady state experiments are used to calculate the rate of steam formation in the core, shutdown will be predicted to occur within less than a millisecond after boiling begins, whereas the SPERT experiments indicated that shutdown requires an order of magnitude larger time than this. This difficulty was circumvented by Forbes by normalisation to experimental data to give an arbitrary constant combining the fraction of the energy release going to steam formation and the area of the fuel plates over which boiling took place. This constant had values in the range 4×10^{-4} to 50×10^{-4} for four reactors considered by Forbes.

The approach provides no insight into the reactor properties which determine the magnitude of this constant. Further, attempts to calculate non–boiling transients under the assumption that b depends only on voiding effects led to large over–estimates of peak powers and energy release, leading to the conclusion that either another mechanism is contributing to shutdown or the magnitude of the void coefficient has been under–estimated by a large amount.

Turner (1968) analysed transient behaviour of two SPERT cores with the inclusion of an analytic form of steam void growth which contained three constants adjusted to give the best fit to all the measured data. Reactivity feedback was assumed to be generated by voiding and expansion only. Good agreement was obtained with experiment for boiling transients but, for non–boiling transients, energy releases were over–estimated by more than a factor of two.

It may be seen from the above that any successful calculation of the SPERT transient results must

(i) Correctly identify non–boiling shutdown effects and use them to calculate values of P_{max}, E_{tm} and E_{tot} in agreement with observed values.

(ii) Include a suitable description of boiling processes to enable energy transfer rates to predict the burst asymmetries observed for boiling transients.

3. REACTOR PHYSICS OF SPERT CORES

As the starting point of the present work, an attempt was made to calculate non–boiling transients with feedback terms derived from static measured values of temperature and void coefficients reported for the SPERT reactors B24/32, B16/40, B12/64 and D12/25 (Figure 1). This approach led to the same order of disagreement with experiment as reported by Forbes (1959) and Turner (1968). Resort was then made to calculation in an attempt to gain some physical insight into the properties of these reactors.

The modular code AUS (Pollard 1974) was used to prepare a four–group cross section set (modules GYMEA, ICPP and EDIT1D) for use in a two–dimensional reactor calculation (module POW). Three regions were used: that defined by the fuelled section of the fuel plates; the region between fuel elements (aluminium + water); and the light water reflector. No account was taken of the presence of control rods and all calculations were performed with a fixed axial buckling corresponding to reflector savings of $\sim$ 15 cm. No attempt was made to 'tune' these calculations by considering more sophisticated cell or reactor representations after the initial calculations were complete. Reactivity coefficients were calculated using a perturbation theory subroutine incorporated in POW. Table 1 shows a comparison of measured and calculated parameters for these SPERT cores. The agreement between them was held to be good enough to demonstrate that no serious errors existed in the calculation.

TABLE 1

COMPARISON OF MEASURED AND CALCULATED REACTOR PARAMETERS

Parameter		B24/32	B16/40	B12/64	D12/25
k_{eff}	calc.	1.044	1.025	1.013	1.060
	expt.	1.046	1.039	1.030	1.060
Max/Av Power [a]	calc.	1.8	2.0	2.3	2.2
	expt.	2.5	2.1	2.2	2.4
C_v ($\%^{-1}$) [b]	calc.	-2.5×10^{-3}	-1.52×10^{-3}	-0.58×10^{-3}	-2.95×10^{-3}
	expt.	-2.8×10^{-3}	-1.70×10^{-3}	-1.05×10^{-3}	-2.52×10^{-3}
$\left(\frac{dk}{d\theta}\right)$ ($^\circ C^{-1}$) [c] (20°C)	calc.	-10.0×10^{-5}	-13.4×10^{-5}	-14.2×10^{-5}	-12.1×10^{-5}
	expt.	-7.7×10^{-5}	-11.9×10^{-5}	-12.6×10^{-5}	-14.7×10^{-5}

(a) Includes average axial distribution given by assumed B_z^2.

(b) Core only perturbation.

(c) Core + reflector temperature perturbation + core only void perturbation corresponding to expansion of water at 20°C/°C.

The published temperature coefficients for the SPERT cores were determined by electrically heating the pool water and establishing uniform core and reflector temperatures with a mechanical stirrer. The temperature dependence of the temperature coefficient obtained in this manner for the 'B' series cores (Whitener 1958) is shown in Figure 2, together with that calculated by POW. Insufficient information is available as to the accuracy of the experiments to enable a quantitative discussion of the differences observed between experiment and calculation but, in broad terms, both show the same weakened dependence of the temperature coefficient with temperature as the core moderation is increased.

For power transients which are fast enough to prevent the transfer of energy from the fuel elements to the reflector, reactivity feedback will be generated only by density and temperature changes in the core. Table 2 shows the results of POW calculations for a temperature perturbation of core and reflector separately. These values do not include any reactivity effect arising from a change of axial buckling or density with temperature. It can be seen that the importance of this neutron spectrum temperature coefficient is greatly enhanced when temperature changes are limited to the core region.

TABLE 2

CORE AND REFLECTOR NEUTRON SPECTRUM TEMPERATURE COEFFICIENTS (x 10^5 $^\circ C^{-1}$)

Region	B24/32	B16/40	B12/64	D12/25
Core	−17.3	−22.6	−24.1	−15.4
Reflector	+ 12.4	+12.8	+11.4	+ 10.0

For analysis of SPERT I transients, void and neutron spectrum temperature coefficients were calculated for typical fuel element positions. The void coefficient variable was changed from volume to temperature by use of the temperature dependent water expansion data given by Turner (1968). These coefficients were then weighted by calculated power factors and summed to give a total core dynamic temperature coefficient consistent with the single cell representation of a reactor in the transient calculation. Table 3 gives the expansion and spectrum components, and the total dynamic temperature coefficient for the four SPERT I reactors, obtained in this way at a temperature of 20 °C.

TABLE 3

COMPONENTS OF DYNAMIC TEMPERATURE COEFFICIENT x 10^5

Component	B24/32	B16/40	B12/64	D12/25
Neutron Spectrum ($°C^{-1}$)	–17.7	–24.5	–29.1	–19.6
Expansion ($°C^{-1}$)	– 5.6	– 3.6	– 1.3	– 6.6
Total	–23.3	–28.1	–30.4	–26.2

Figure 3 shows the temperature dependence of the total temperature coefficient calculated for these cores. A linear relationship with temperature was fitted by eye for use in the transient analysis.

4. CALCULATION OF SPERT TRANSIENTS

The code ZAPP (B.E. Clancy, AAEC unpublished report) solves the reactor kinetic equations with a time dependent multiplication factor, k(t), and the coupling equation given by the one–dimensional heat transfer Equation

$$\frac{\partial}{\partial t}\left[C(\theta,x)\,\theta(x,t)\right] = \frac{\partial}{\partial x}\left[K(\theta,x)\,\frac{\partial}{\partial x}\,\theta(x,t)\right] + S(x)\ , \qquad (9)$$

and

$$k(t) = k_o + \int_0^L dx \int_{\theta_o}^{\theta(x,t)} \frac{dk}{d\theta}(x,\theta)\,d\theta\ , \qquad (10)$$

where

C = specific heat, K = thermal conductivity } values taken from Houghtaling, Sola & Spano (1964),

θ = temperature,

S = heat source = average fission density, and

L = width of unit cell.

ZAPP has been used to calculate non–boiling SPERT transients. The reactor was represented by a unit cell comprising fuel alloy, cladding and water moderator. Fourteen water regions, each 0.003 cm wide, were adjacent to the cladding and four water regions spanned the remainder of the water channel. The power density in the cell was made equal to the core average power density and partitioned between fuel alloy, cladding and water according to the data of Houghtaling, Sola & Spano (1964). The water regions were assigned a dynamic temperature coefficient by multiplying the total values shown in Table 3 by the ratio of the width of the region to that of the whole

water channel. It follows that, since the total dynamic temperature coefficient is similar for all four reactors, the one with the narrowest water channel will have the largest reactivity feedback coefficient in regions adjacent to the cladding.

Expansion of the fuel plates was included as a linear expansion of the plate thickness only, for it is not clear that cubical expansion should be used since the SPERT fuel plates are not constrained within the fuel assemblies. Since this effect is only 10 per cent of the total feedback for the core with the largest void coefficient, even when cubical expansion is assumed, it is not of critical importance.

Table 4 gives other core parameters of interest in the transient analysis.

TABLE 4

PARAMETERS FOR SPERT CORES

Parameter		B24/32	B16/40	B12/64	D12/25
Prompt life time ℓ^*	(μs)	50	70	77	60
β_{eff}		0.007	0.007	0.007	0.007
Water gap	(cm)	0.165	0.165 (alt) 0.482	0.483	0.457
No. of fuel elements		32	40	64	25
Fuel plates/element		24	16	12	12
^{235}U/fuel plate	(g)	7.0	7.0	7.0	14.0
Cladding thickness	(cm)	0.0508	0.0508	0.0508	0.0508
Alloy thickness	(cm)	0.0508	0.0508	0.0508	0.0508
Vol. aluminium	(ℓ)	58.6	53.2	69.4	34.0
Vol. water	(ℓ)	52.5	85.6	153.0	52.0

4.1 Simulation of Boiling Effects in SPERT Transients

Once the cladding reaches the saturation temperature of water, the onset of boiling will alter the heat transport process from cladding to water. It is of interest to identify the transition region from non–boiling to boiling shutdown processes.

The energy E_b required to raise the 'hot spot' of the cladding to saturation temperature is

$$E_b \sim \frac{H_{fp}\,\Delta\theta}{F\,\zeta} \quad , \tag{11}$$

where H_{fp} = heat capacity of fuel plates,

$\Delta\theta$ = initial water sub–cooling,

F = core power factor, and

ζ = fraction of energy remaining in the fuel plates.

If boiling at the core hot spot has just commenced at the time of peak power and is assumed to occur when the cladding has reached saturation temperature,

$$\left(\frac{\delta k}{k}\right)_c \sim (1 - \zeta) \frac{E_b}{H_w} \frac{dk}{d\theta} \quad , \tag{12}$$

where $\left(\frac{\delta k}{k}\right)_c$ = compensated reactivity at peak power,

H_w = heat capacity of water, and

$\frac{dk}{d\theta}$ = average temperature coefficient of reactivity.

Then, substituting Equation (11) into Equation (12)

$$\left(\frac{\delta k}{k}\right)_c \frac{\zeta}{1-\zeta} = \frac{H_{fp}}{H_w} \frac{\Delta\theta}{F} \frac{dk}{d\theta} \quad . \tag{13}$$

The left hand side of the equation may be calculated as a function of α_o by ZAPP and is shown in Figure 4. The right hand side is a property of the reactor and determines for which value of α_o boiling will commence at the core centre at the time of peak power. These values of α_o are shown in Figure 3 for an assumed value of $\Delta\theta$ of 80 °C. Approximate experimental values are shown in parenthesis. For all α_o greater than these values, boiling processes will contribute to reactor shutdown, and it is necessary to include this in the calculations.

Previous attempts to calculate boiling shutdown have considered that only void coefficients provide reactivity feedback. This necessitates a description of the rate of void growth. The present work indicates that the void coefficient is unlikely to be the major contributor to reactor shutdown. If it is further assumed that bubble agitation at the boundary of cladding and water acts as a very efficient means of heat transport to the water at a lower temperature and that the volume of these bubbles is relatively small, then an increased rate of reactivity feedback will occur, as energy stored in the fuel plate is transferred rapidly to the water beyond the cladding–water boundary.

On this basis, the temperature dependent conductivity data for water in the ZAPP calculations were entered as 1.0 when the temperature equalled the initial sub–cooling of the water divided by the core power factor. (Subsequently it was shown that the results were relatively insensitive to the conductivity assigned to boiling water provided it was large compared with 0.0016, the conductivity of water below the boiling point. Making the boiling conductivity 0.1 instead of 1.0 changed P_{max} by 6 per cent and E_{tm} by 10 per cent. Similarly, changing the temperature at which boiling commenced by 10 °C changed P_{max} by 10 per cent and E_{tm} by 6 per cent.)

This model results in the rapid propagation of a temperature front into the water once the temperature of the cladding reaches the saturation temperature of water, and a reactivity feedback time constant shorter than that of the energy input. Prior to reaching saturation temperature, the cladding temperature is increasing with an exponential time constant approximately equal to α_o and the coolant temperature distribution has a relaxation length of $\sqrt{\frac{K}{\alpha_o C}}$. In the calculations, once the coolant in the regions close to the cladding begins switching to the high conductivity 'boiling' state, the following situation applies:

- The rate of rise of cladding temperature begins to fall.
- After 'boiling' has been in progress for time t, the cladding temperature front will have advanced into the coolant a distance vt, where v is the approximately constant velocity of propagation of the temperature front.

- Because of the very rapid rise in temperature of a coolant region when the conductivity is made large, the immediately adjacent non–boiling regions will have a temperature distribution whose relaxation length is $<< \sqrt{\frac{K}{\alpha_o C}}$

- The remainder of the coolant channel will have the same temperature distribution it had prior to boiling.

It can be shown that, subject to certain approximations, the reactivity feedback will be dominated by the 'boiling' regions shortly after boiling commences, and is approximately proportional to $vt \exp(\alpha_o t)$. The fractional rate of increase in feedback reactivity is then given by $\frac{1}{t} + \alpha_o$.

The actual feedback calculated by ZAPP is shown in Figure 5 for core B24/32 and initial inverse periods of 10, 30, 50 and 100 s^{-1}. The time is plotted with zero as the time of peak power and in units of $\alpha_o t$.

It can be seen that for $\alpha_o < 30$, the feedback prior to peak power is increasing at the same rate as the energy; for $\alpha_o > 30$ the increased rate of transport of energy to the water leads the reactivity feedback to increase almost twice as fast. This is in accord with the SPERT modification to the Nordheim–Fuchs equation, where the feedback was made proportional to the square of the energy to reproduce the observed pulse asymmetries.

5. RESULTS OF SPERT CALCULATIONS

Parameters calculated by ZAPP are shown, together with the corresponding experimental data in Figures 6 – 13.

5.1 Discussion of Results

Figure 14 shows the ratio of calculated maximum powers and energy releases at the time of peak power to their experimental values. These ratios are contained between 0.8 and 1.2 and indicate a slight tendency to increase from 0.8 as α_o increases. This may be caused by energy loss through processes not included in the ZAPP calculation, such as convection in the water and heating of structural parts of the core by conduction.

It is difficult to quantify the discussion of the significance of the level of agreement reached between experimental and calculated data chiefly because of the lack of error assignments to many measured SPERT parameters. Haire (1958) quotes ± 5 per cent uncertainty in the power calibration of the 'B' cores and Zeissler (1963) gives ± 2.5 per cent for the D12/25 core. Energy release data were obtained by numerical integration of the transient power traces, and it may be supposed that any error introduced by this procedure would be small and systematic. Fuel plate temperature measurement techniques are claimed by Spano & Miller (1962) to be capable of following a 2 ms period temperature rise with less than 5 per cent lag, and the temperature rise itself is determined within 1°C. However, fuel plate temperature will depend on local conditions surrounding the thermocouple and the location within the core; comparison of calculation with such an intensive parameter is made difficult.

The accuracy of the calculated feedback terms can only be assessed by comparison of the same calculational method against a measured parameter such as the whole reactor temperature coefficient. However, the experimental accuracy is not given for most SPERT static measurements. The largest disagreement with an experimental number is for the void coefficient for B12/64.

Features of the comparison of experimental and calculated data for the individual cores are noted in Section 5.2 *et seq.*

5.2 SPERT B24/32

Figure 6 indicates reasonable agreement between experiment and calculation for P_{max} and E_{tm}, except for α_o values between 10 and 40 s^{-1}. Comparison of temperature data is obscured by the large corrections (indicated by arrows and made by the authors on the basis of flux distributions reported by Wagner (1957)) made to data measured away from the core centre.

The onset of 'boiling' shutdown for $\alpha_o > 40$ is shown clearly in the decrease in the rate at which E_{tm} increases with α_o. Because of the small coolant channel width, feedback in regions close to the fuel plate is large and the 'boiling' front is not required to advance very far to halt the power rise.

Examination of Figure 10 shows that the ratio $\alpha_o E_{tm}/P_{max}$, which is an indication of the rate of negative reactivity feedback relative to energy input, is poorly represented by the calculation for $\alpha_o < 40$. The low measured values in this range indicate a markedly non–linear shutdown mechanism, which cannot be boiling since the experimental fuel plate temperatures have not reached the saturation temperature of water. Shown also in Figure 10 is the variation of $\alpha_o E_{tm}/P_{max}$ with α_o for a Nordheim–Fuchs burst (*i.e.* with feedback coupled directly to energy release) as computed by ZAPP. The differences observed between this model and the ZAPP calculation, with heat transfer providing the reactivity coupling, suggest a time delay between the release of energy in the fuel plate and the generation of reactivity feedback in the coolant.

5.3 SPERT B16/40

Although there is less extensive experimental data for this core, Figures 7 and 10 indicate good agreement between experiment and calculation for the parameters P_{max}, E_{tm}, θ_{tm} and $\alpha_o E_{tm}/P_{max}$. Because the coolant channels in this core alternated between 0.165 and 0.483 cm widths, a full cell representation in ZAPP was necessary. At that time the number of 'regions' in the code was limited to twenty and this required that fewer small water regions be used near the fuel plate. This has produced the upturn in the data for $\alpha_o > 50$.

5.4 SPERT B12/64

This reactor has the smallest void coefficient contribution to the reactivity coefficient of the four reactors analysed in this report, and the assumption that boiling induced voids can be neglected is reasonable. Figures 8 and 10 show good agreement with experiment except for values of E_{tm} in the region of $\alpha_o = 10$ and the two values for $\alpha_o < 0.2$.

5.5 SPERT D12/25

Unlike the 'B' series reactors, this core contained fuel elements with 14 instead of 7 g ^{235}U per fuel plate. This means that although the dynamic reactivity temperature coefficient is about the same as B24/32, the width of the water channel is comparable to B12/64. Thus, since the boiling model satisfactorily reproduced B12/64 experimental data in the boiling shutdown region, D12/25, with a large void coefficient component of the total dynamic temperature coefficient and a requirement that the 'boiling' temperature front propagate much further than in B24/32, affords a good test of the validity of neglecting steam formation.

Figure 9 shows that for $\alpha_o > 60$, ZAPP increasingly overpredicts all three measured parameters. For $\alpha_o = 100$, the boiling model temperature front must advance 0.035 cm into the coolant compared with 0.015 cm for a similar transient in B24/32; shutdown is correspondingly delayed. The experiments suggest that steam void formation is contributing markedly to shutdown for $\alpha_o > 60$.

Inspection of the data in Figure 9 shows that the reproducibility of power bursts is certainly outside the range of ±2.5 per cent given for the power calibration. This is not unexpected because of the many variables involved in the shutdown mechanism. Beyond $\alpha_o = 150$, core structural damage such as partial fuel plate melting was reported, but it is not possible to ascertain whether this occurred before or after peak power.

Figure 10 indicates good agreement between the experimental data and calculated values of $\alpha_o E_{tm}/P_{max}$. The comparison of E_{tot}/E_{tm} values in Figure 11 shows clearly that the calculated transients are not maintaining a high enough rate of feedback to produce the observed pulse asymmetries for large α_o. (E_{tot} values are reported for D12/25 but not for the 'B' series cores; the values shown for these have been obtained by using a planimeter on the published power traces and are not very accurate.)

5.6 SPERT B12/64 Ramp Tests

Ramp addition of reactivity experiments reported by Neal (1959) cover ramp rates from 10^{-4} $\delta k/k\ s^{-1}$ to 3.3×10^{-3} $\delta k/k\ s^{-1}$ and reactor powers at the time of ramp initiation from 1 mW to 11 kW.

Figure 12 shows a comparison of measured and calculated maximum inverse period as a function of initial reactor power. There is an unfortunately wide scatter in the experimental data and no indication of the likely error in either ramp rate or in the determination of α_{max}, but the calculations show the same weak dependence of α_{max} on initial power and proportionality to ramp rate.

Figure 13 shows P_{max} as a function of α_{max} for calculation and experiment. Also shown is the relationship between P_{max} and α_o for the step tests previously calculated. It can be seen that when the ramp produces a superprompt critical excursion, the approximation that the peak power is the same as that for a step insertion of reactivity with $\alpha_o = \alpha_{max}$ is a good one.

6. CONCLUSIONS

The general level of agreement obtained with experiment for calculated power transients in four SPERT cores supports the case that discrepancies in calculations of non–boiling power transients have arisen because of the neglect of positive temperature coefficients in the reflector.

A simple model of boiling shutdown, involving the collapse of the non–boiling temperature distribution in the coolant channel and neglect of steam–produced voids, has been tested and found to give a satisfactory description of SPERT transient data. Although SPERT burst shapes may be reproduced by a variety of postulated models, it is believed that the present results, which also give good agreement with observed peak powers without recourse to normalisation, indicate that the actual physical processes are being reasonably modelled. This conclusion, however, must be qualified if the timescale of the power burst is sufficiently long for the production of large steam voids, or if the onset of film boiling inhibits the transfer of heat from the fuel plate to the coolant. In the former case, the calculational method described will over–estimate the energy release and in the latter, it will under–estimate it.

7. ACKNOWLEDGEMENTS

The authors are grateful to J.P. Pollard and G. S. Robinson for advice and assistance in running the code AUS.

8. REFERENCES

Forbes, S. G. (1959) – in Quarterly Progress Report, IDO 16489 (ed. G. O. Bright) p. 71.

Haire, J. C. (1958) – in Quarterly Progress Report, IDO 16452 (ed. G. O. Bright) p. 32.

Houghtaling, J.E., Sola, A. & Spano, A. (1964) – Transient temperature distributions in the SPERT I D12/25 fuel plates during short period power excursions. IDO 16884.

Neal, W. J. (1959) – in Quarterly Progress Report, IDO 16489 (ed. G. O. Bright) p. 11.

Pollard, J. P. (1974) – AAEC/E269, Appendix A.

Spano, A. H. & Miller, R. W. (1962) – SPERT I destructive test program safety analysis. IDO 16790.

Turner, W. J. (1968) – Calculations of SPERT transients. *J. Nucl. Energy*, 22: 397–409.

Wagner, R. (1957) – in Quarterly Progress Report, IDO 16416 (ed. G. O. Bright) p. 20.

Whitener, H. (1958) – in Quarterly Progress Report, IDO 16437 (ed. G. O. Bright) p. 12.

Wing, A. P. (1964) – Transient test of the fully enriched, aluminium plate type B cores in SPERT I. IDO 16964.

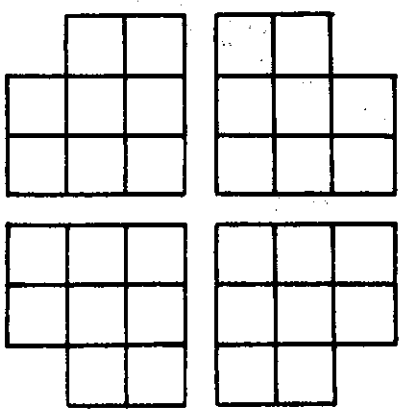

B24/32

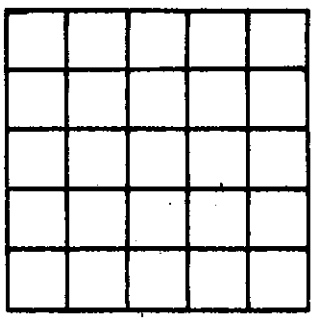

D12/25

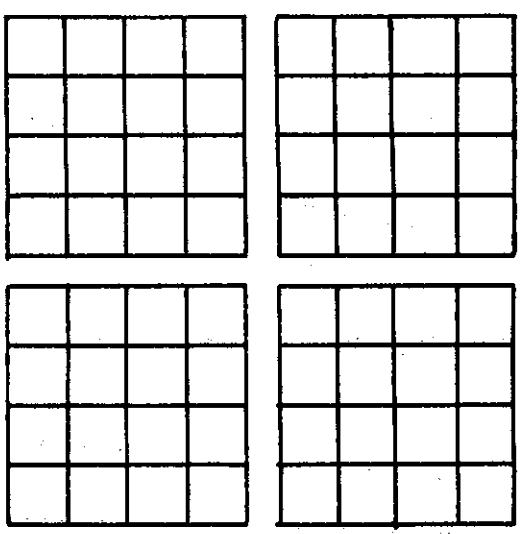

B12/64

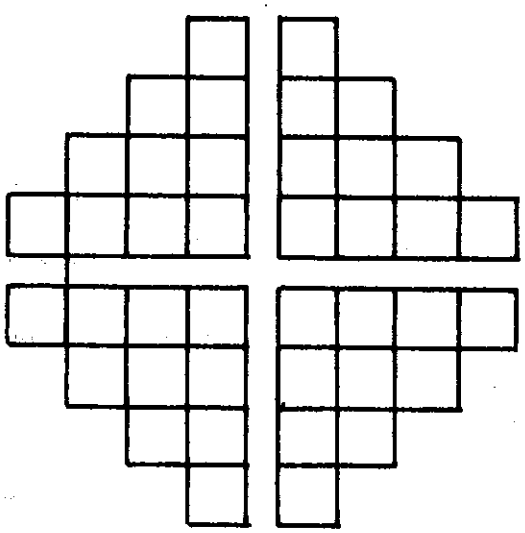

B16/40

FIGURE 1. SPERT 1 CORE GEOMETRIES

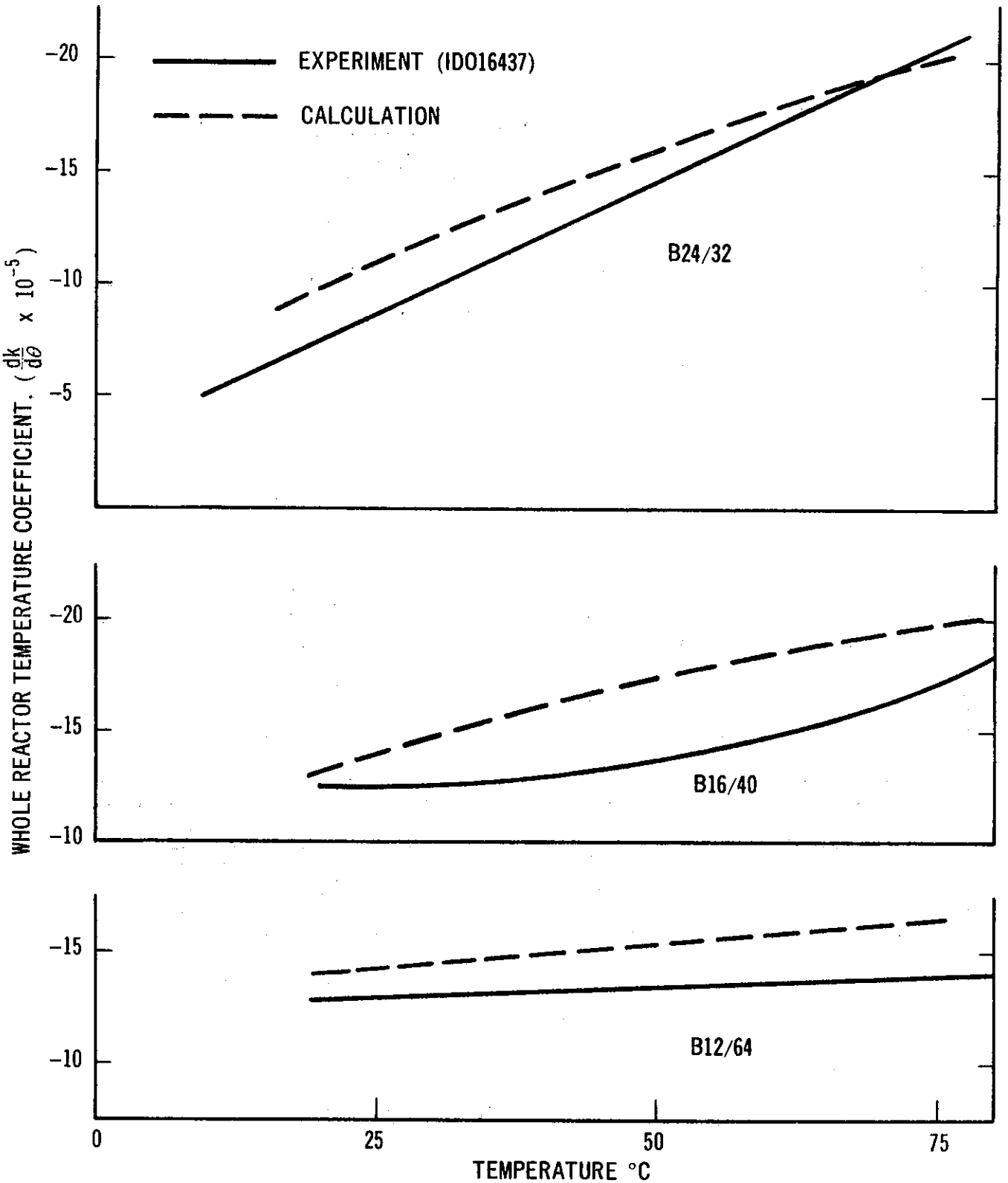

FIGURE 2. TEMPERATURE DEPENDENCE OF WHOLE REACTOR TEMPERATURE COEFFICIENT OF REACTIVITY FOR 'B' SERIES CORES

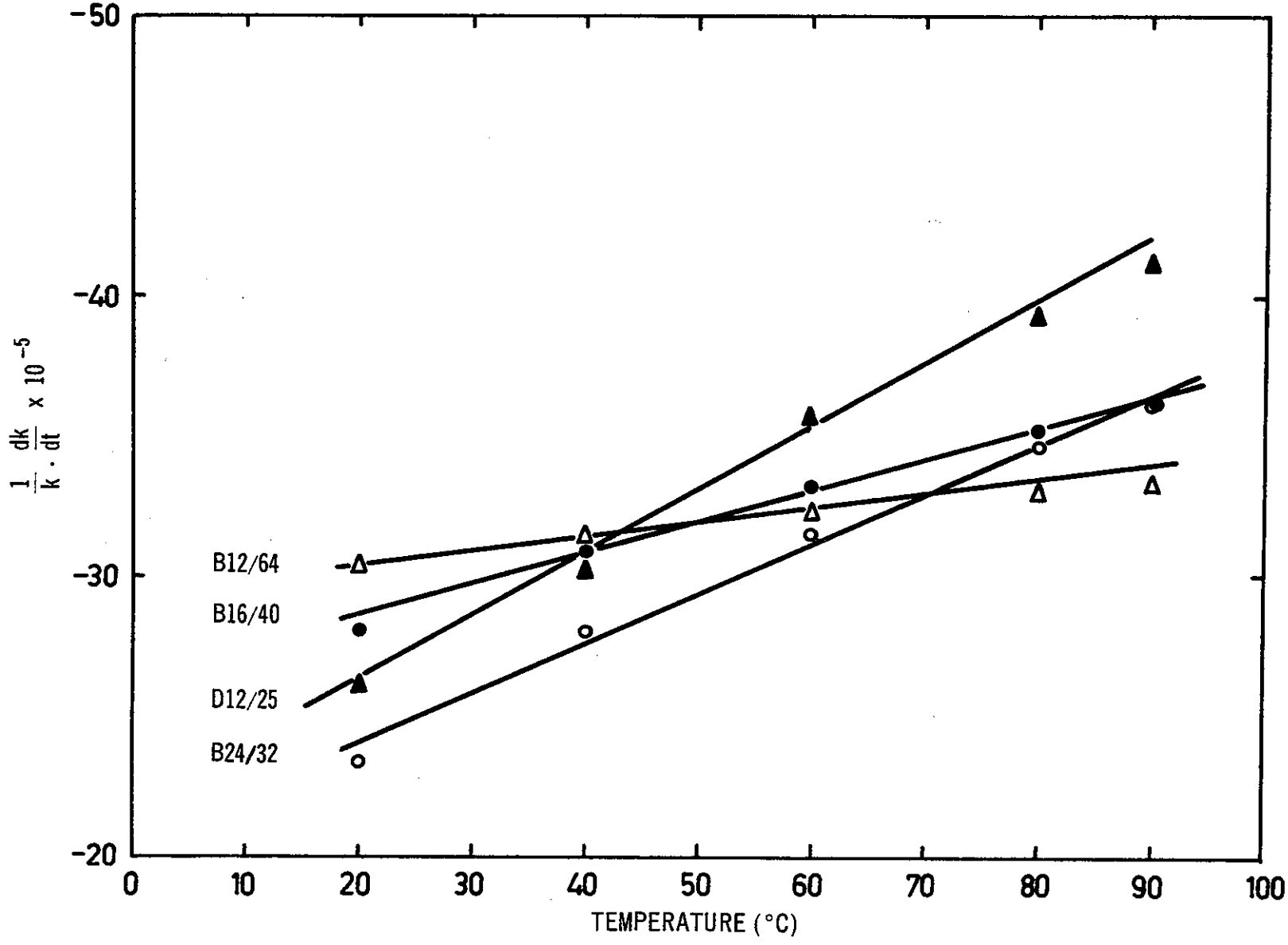

FIGURE 3. TEMPERATURE DEPENDENCE OF TEMPERATURE COEFFICIENT USED IN ZAPP CALCULATIONS

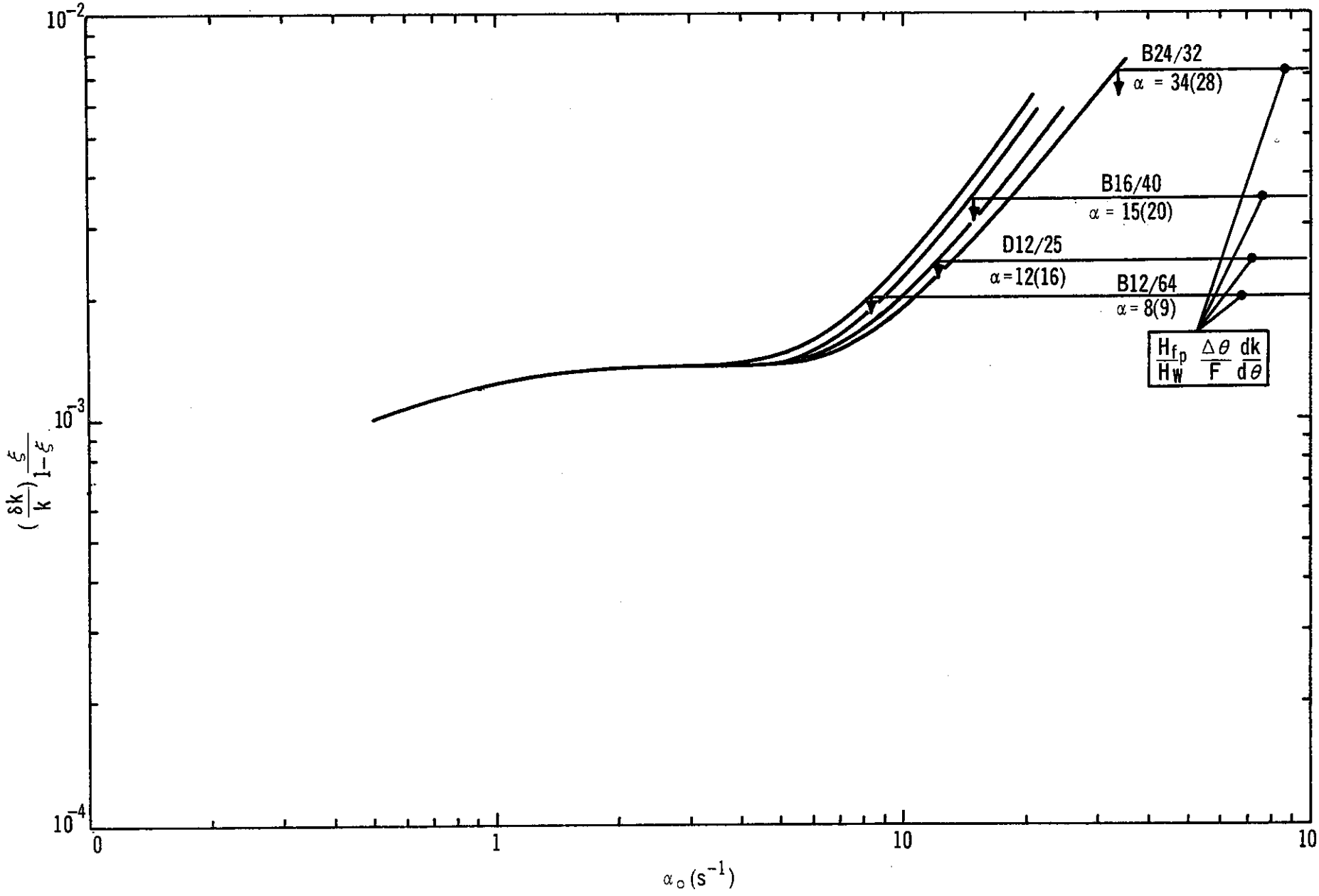

FIGURE 4. INITIAL INVERSE PERIOD TO PRODUCE BOILING AT TIME OF PEAK POWER

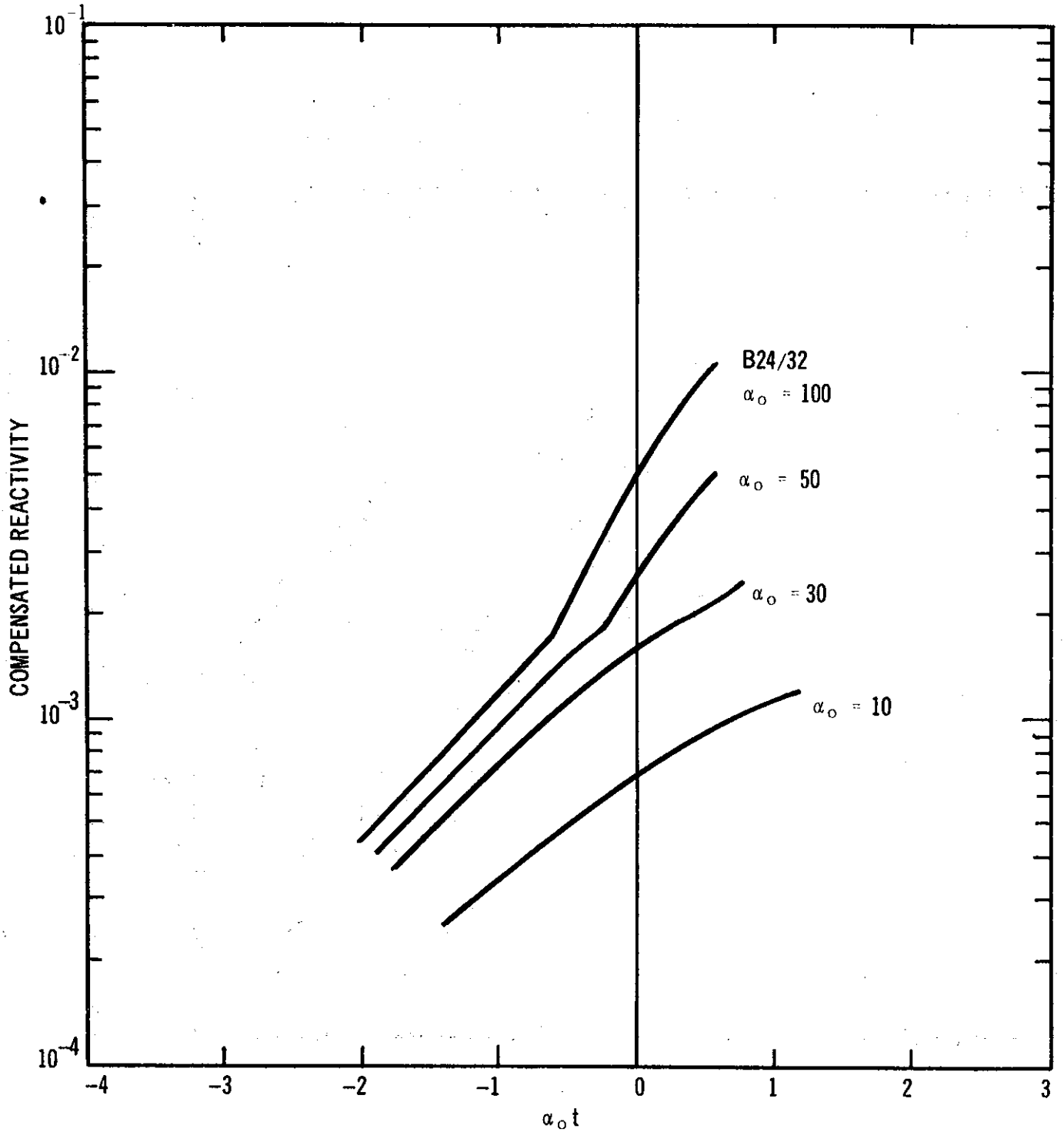

FIGURE 5. REACTIVITY COMPENSATION FOR BOILING AND NON-BOILING TRANSIENTS

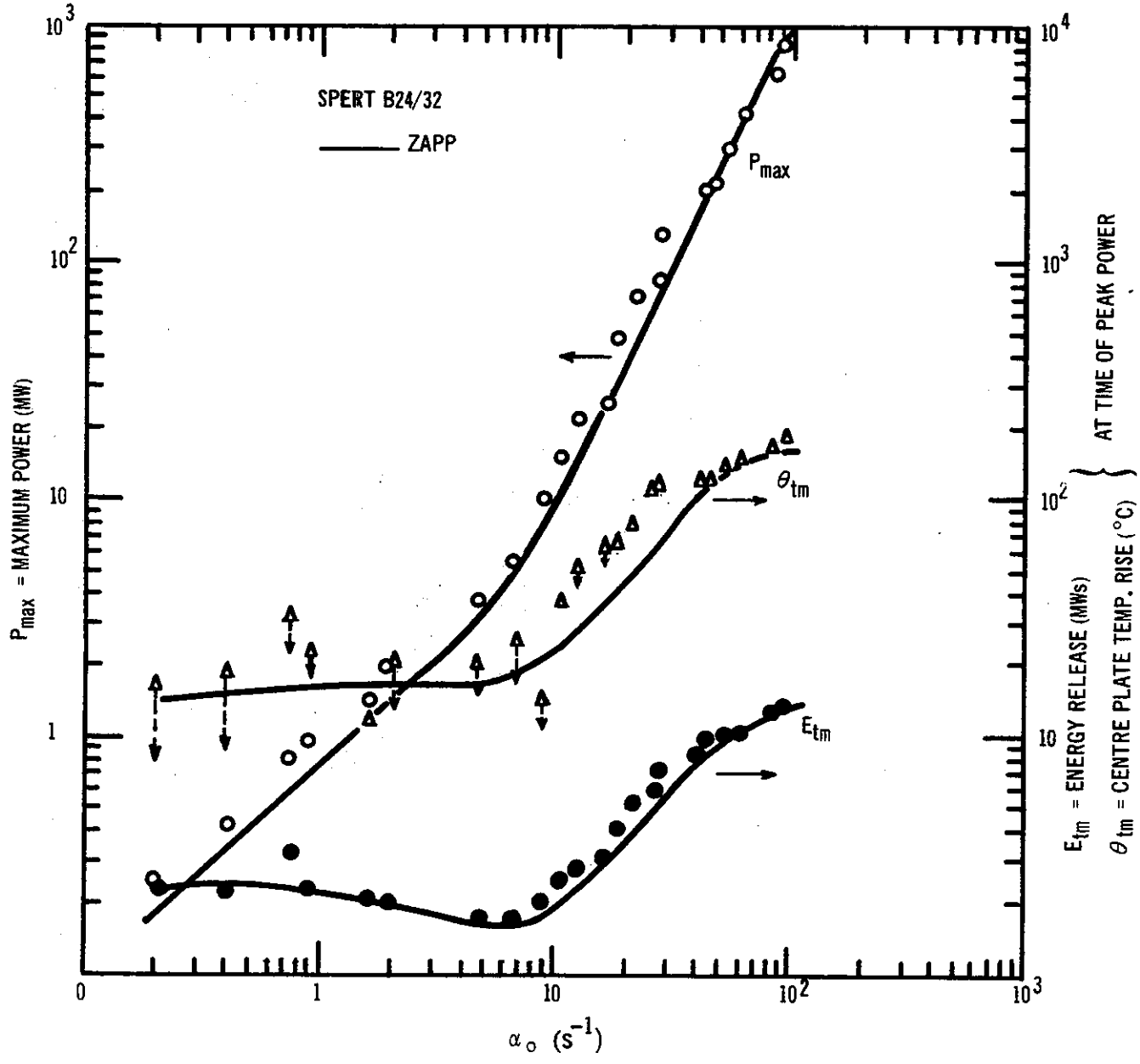

FIGURE 6. CALCULATED AND EXPERIMENTAL TRANSIENT DATA, SPERT B24/32

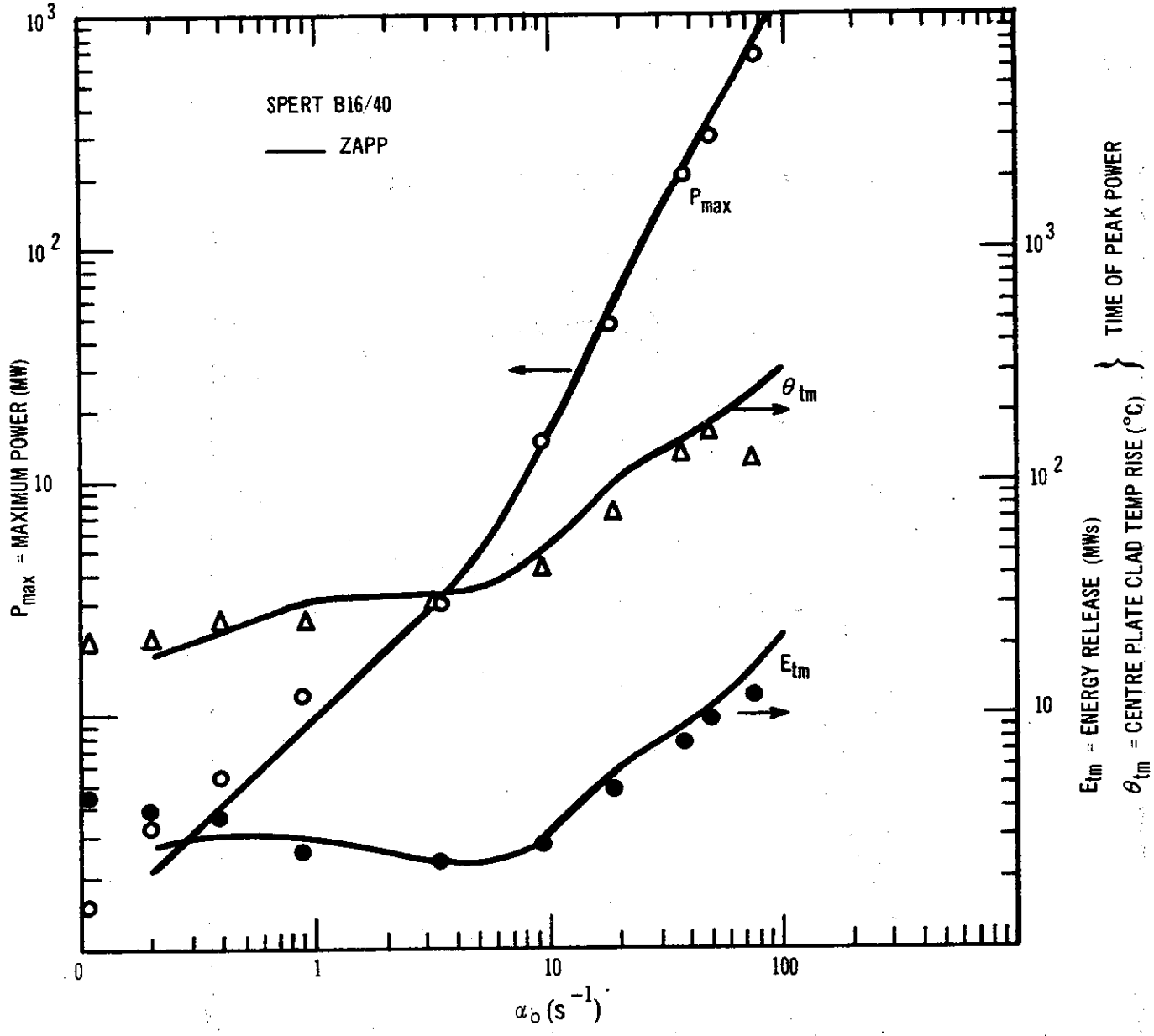

FIGURE 7. CALCULATED AND EXPERIMENTAL TRANSIENT DATA, SPERT B16/40

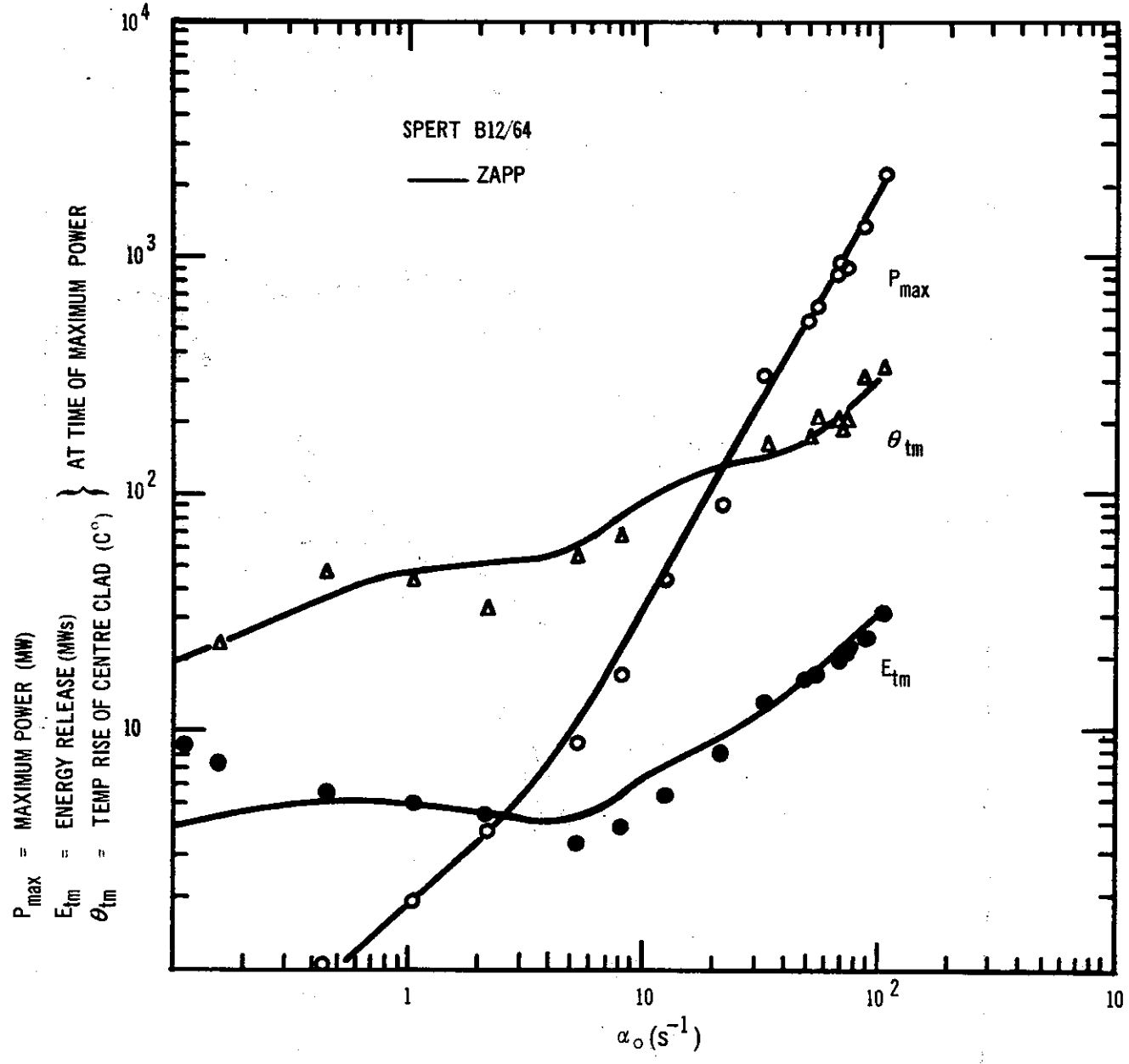

FIGURE 8. CALCULATED AND EXPERIMENTAL TRANSIENT DATA, SPERT B12/64

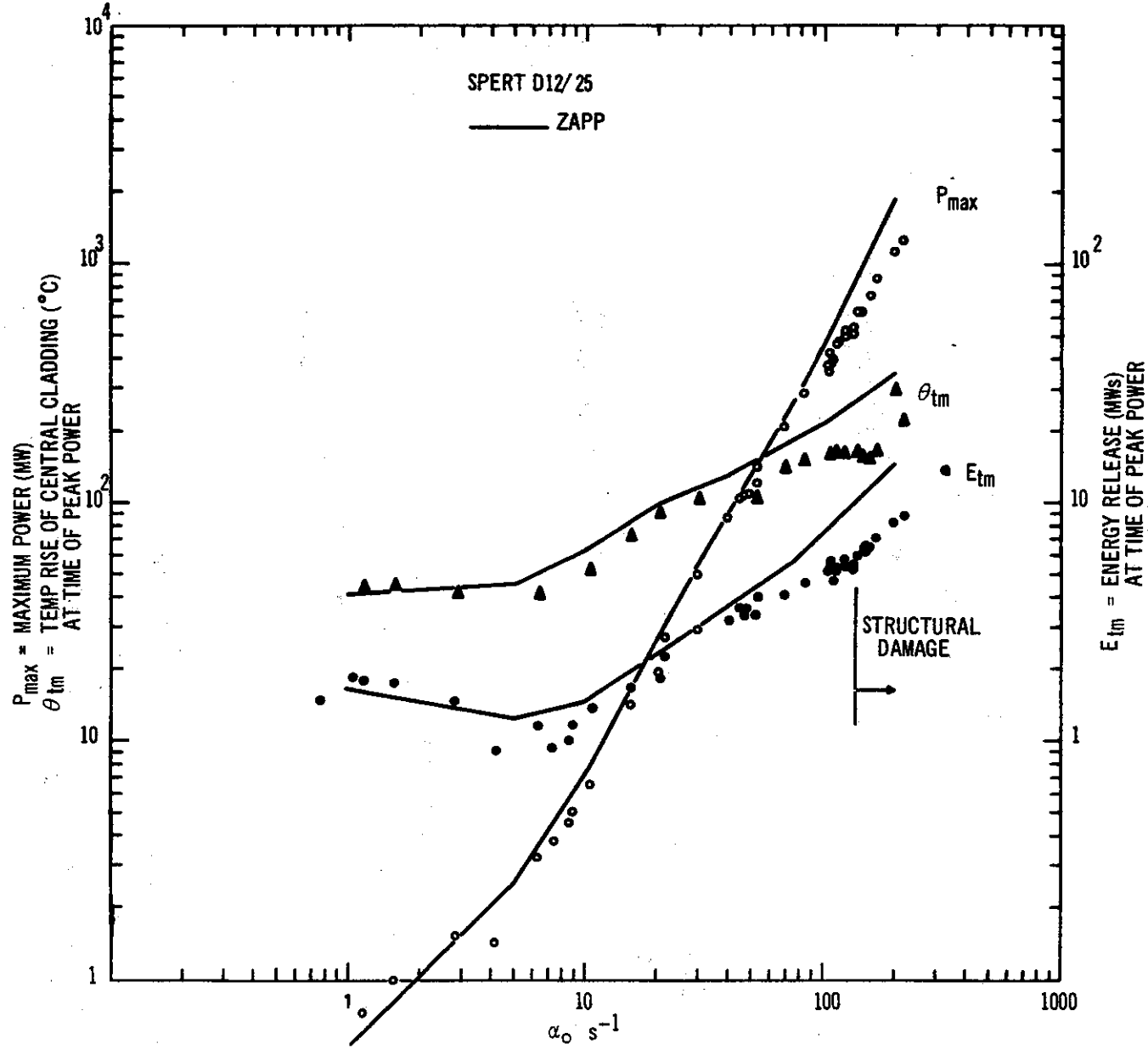

FIGURE 9. CALCULATED AND EXPERIMENTAL TRANSIENT DATA, SPERT D12/25

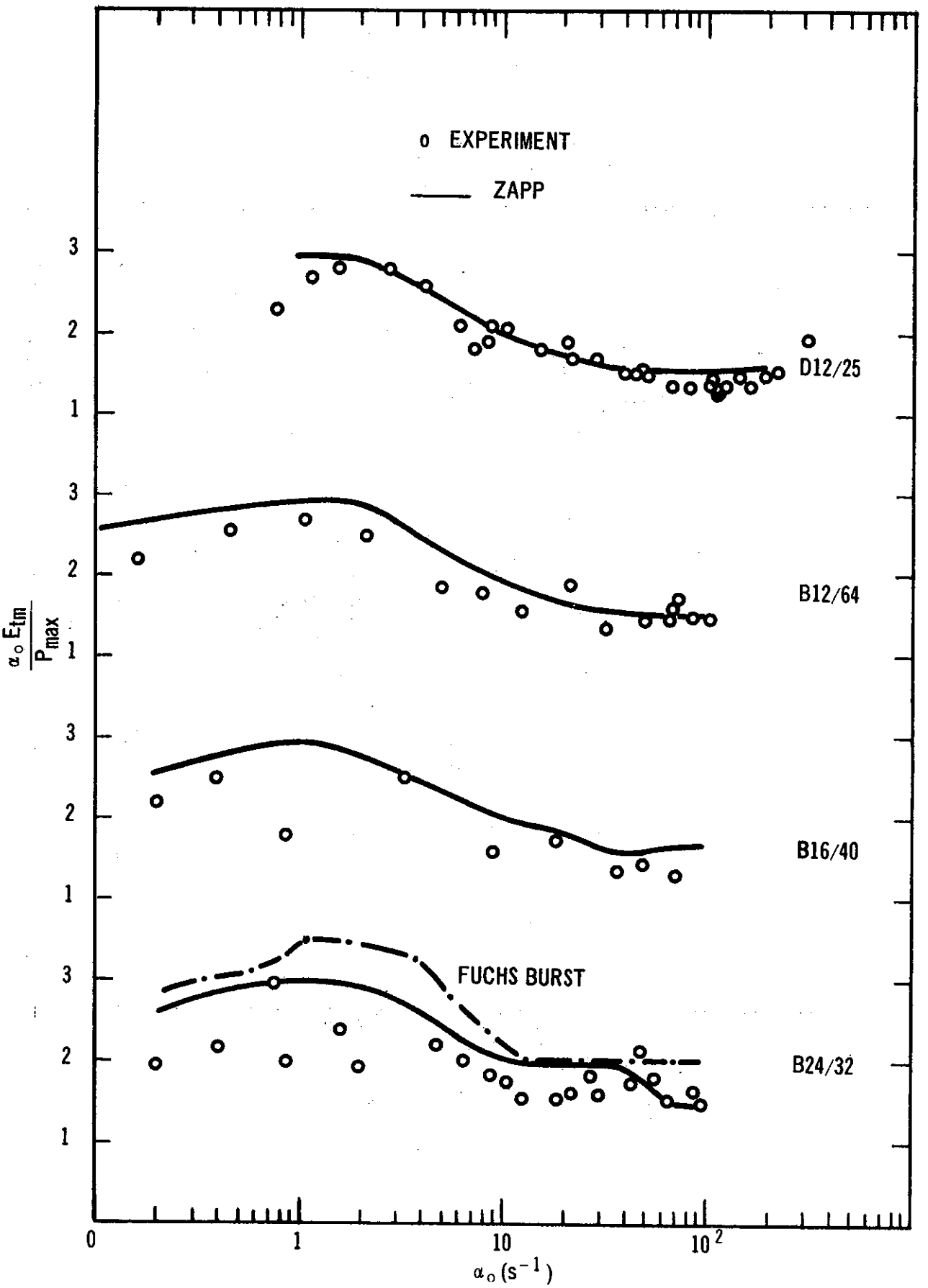

FIGURE 10. SPERT BURST SHAPES TO TIME OF PEAK POWER

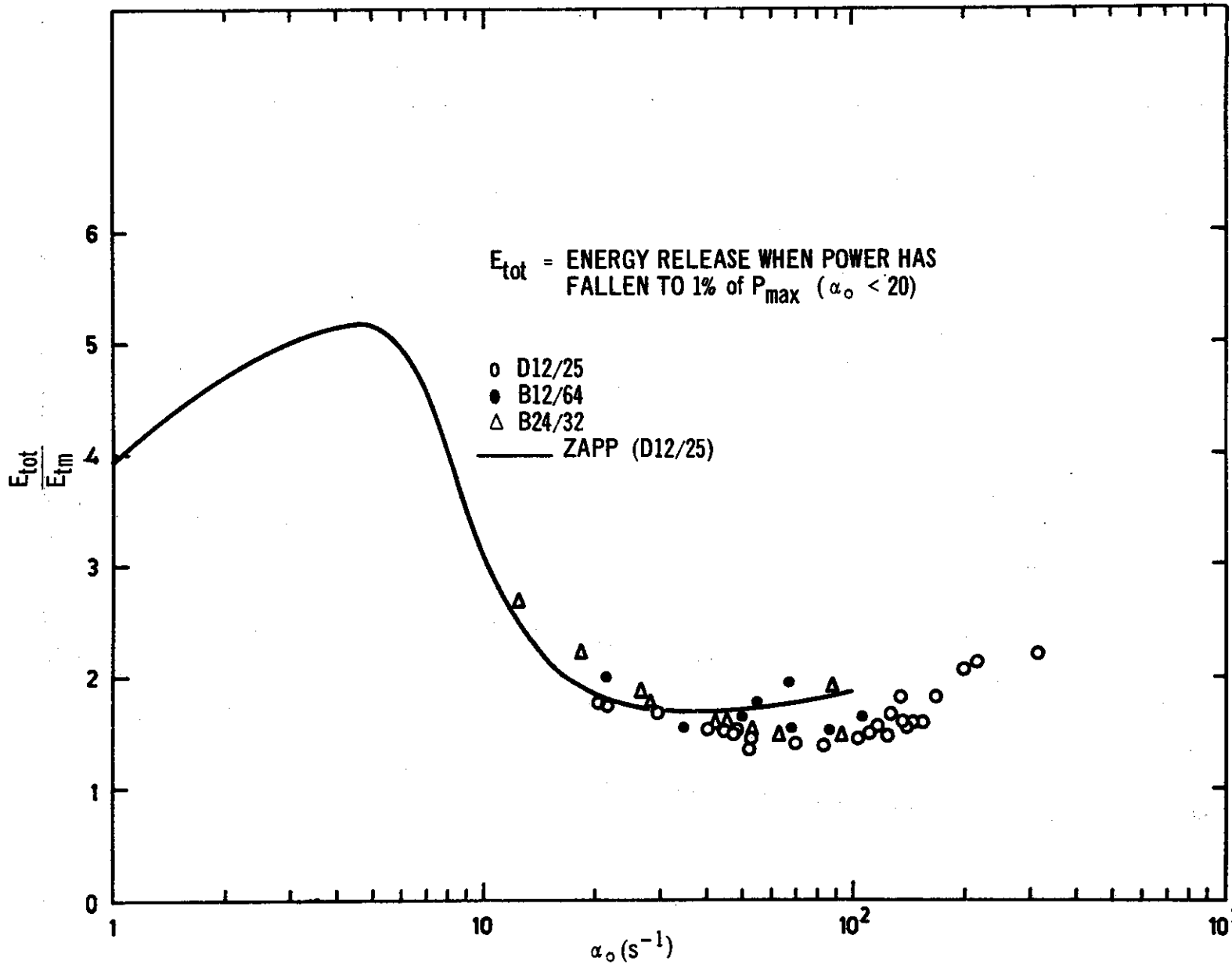

FIGURE 11. SPERT BURST SHAPE ASYMMETRY

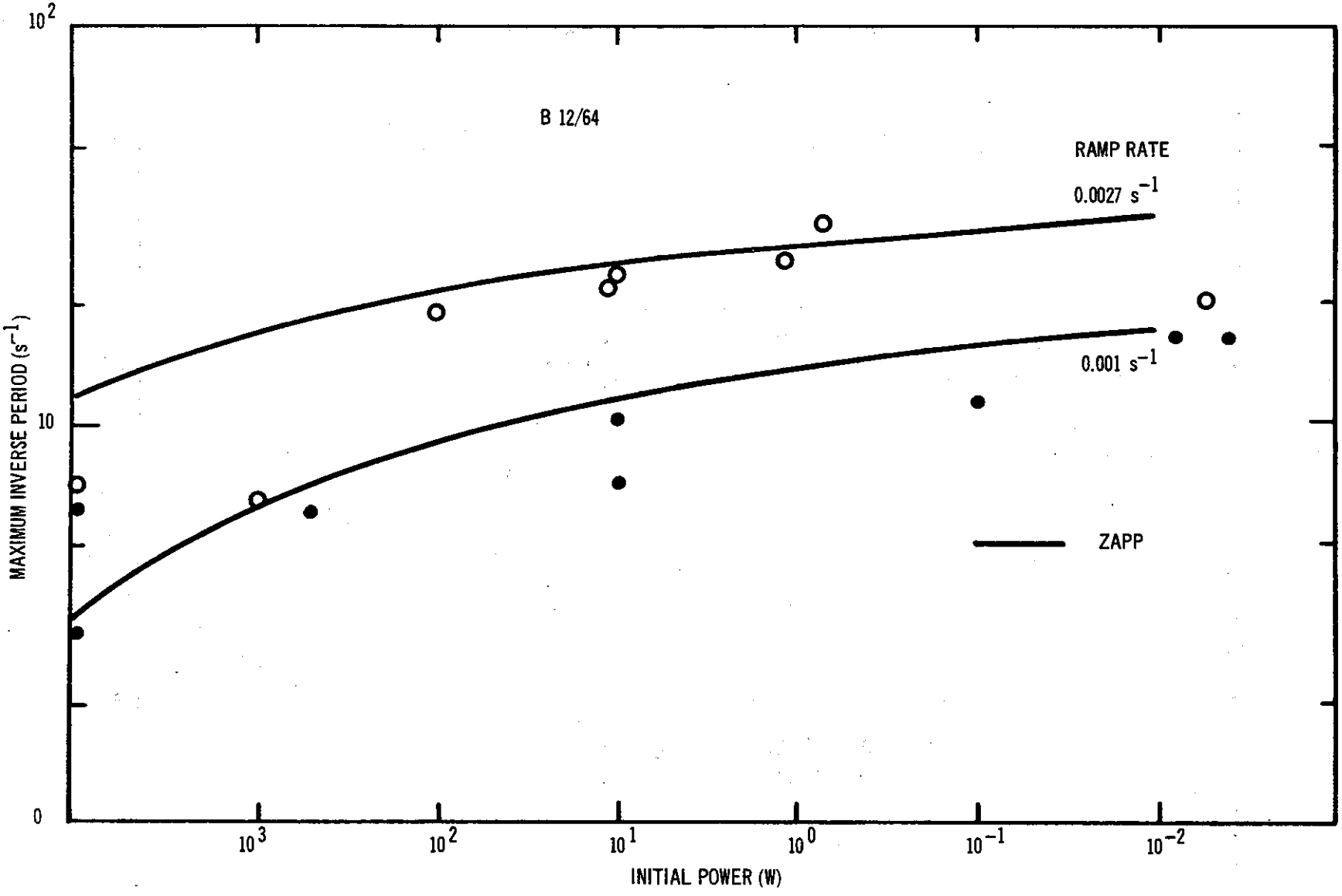

FIGURE 12. MAXIMUM INVERSE PERIOD FOR RAMP EXCURSIONS, B12/64

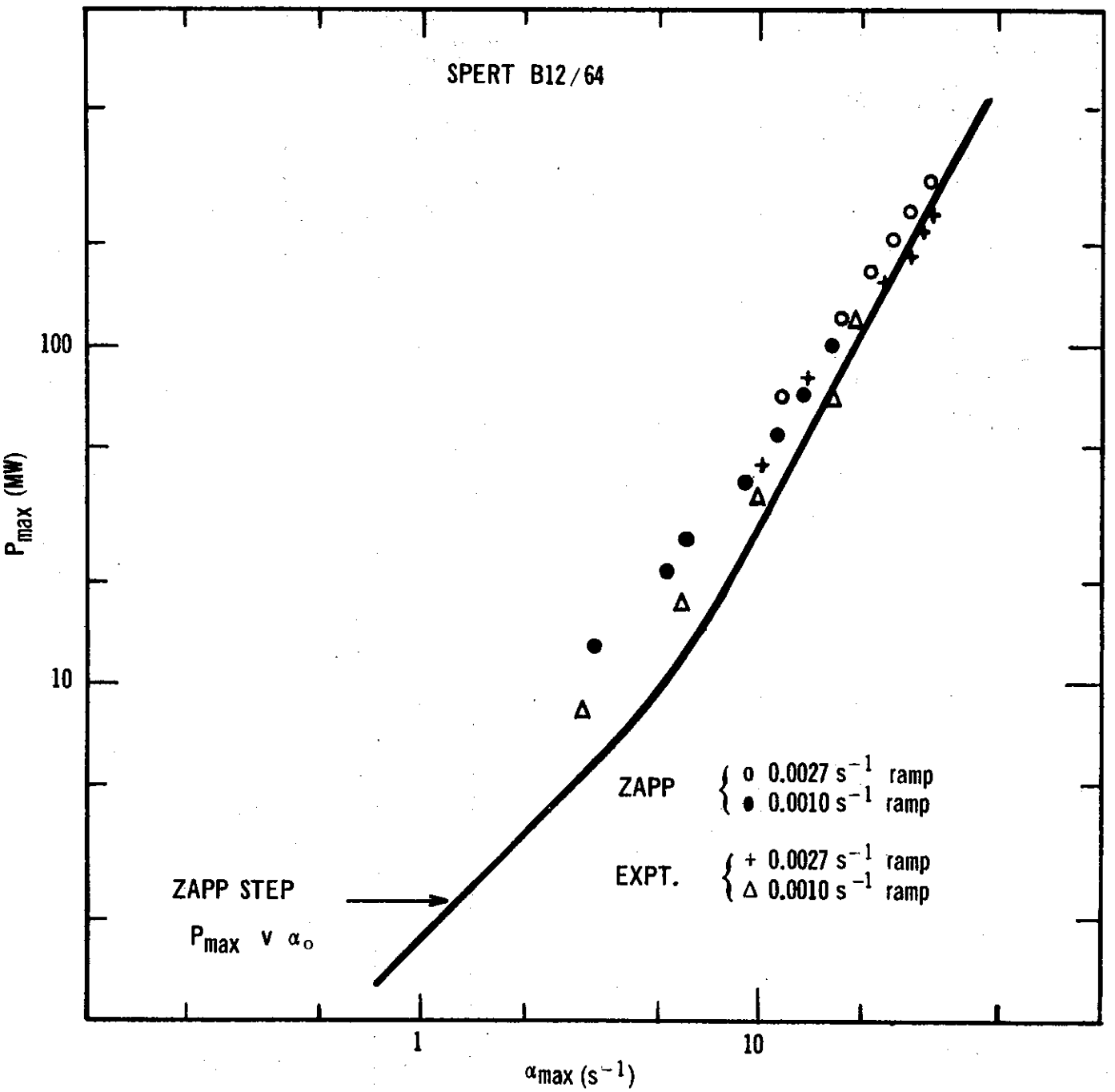

FIGURE 13. MAXIMUM POWER FOR RAMP EXCURSIONS, B12/64

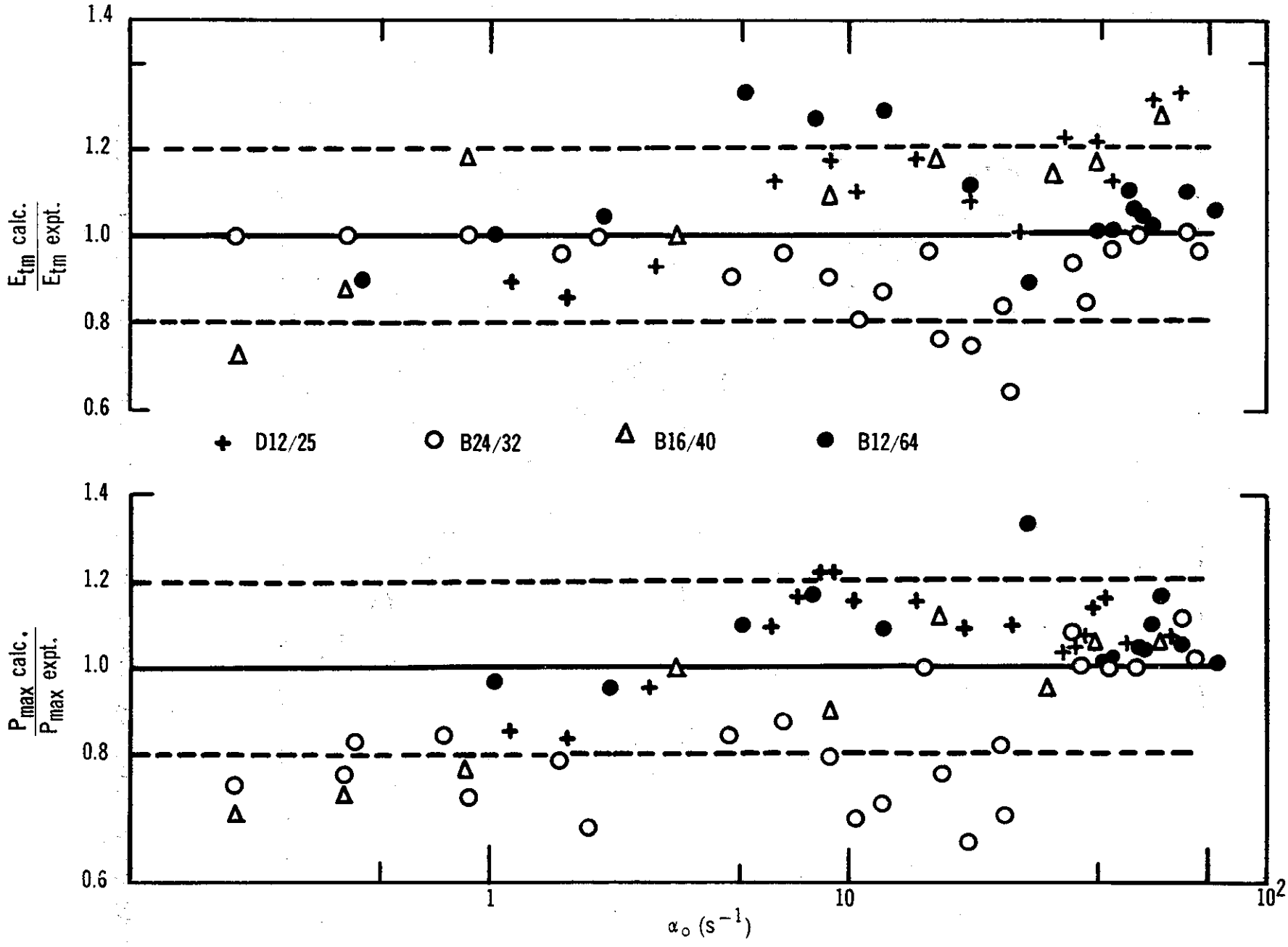

FIGURE 14. RATIOS OF MEASURED AND CALCULATED POWERS AND ENERGY RELEASED

ERRATUM

AAEC/E345

by

B. E. CLANCY
J. W. CONNOLLY
B. V. HARRINGTON

The following entry is omitted from the Reference listing:

Zeissler, M. J. (1963) – Non–destructive and destructive transient tests of the SPERT 1D core. IDO 16886.